

# Platelet interaction with von Willebrand factor is enhanced by shear-induced clustering of glycoprotein Ib $\alpha$

Eelo Gitz,<sup>1</sup> Charlotte D. Koopman,<sup>1</sup> Alèkos Giannas,<sup>1</sup> Cornelis A Koekman,<sup>1</sup> Dave J. van den Heuvel,<sup>2</sup> Hans Deckmyn,<sup>3</sup> Jan-Willem N. Akkerman,<sup>1</sup> Hans C. Gerritsen,<sup>2</sup> and Rolf T. Urbanus<sup>1</sup>

<sup>1</sup>Thrombosis and Haemostasis Laboratory, Department of Clinical Chemistry and Haematology, University Medical Center Utrecht, <sup>2</sup>Department of Molecular Biophysics, Utrecht University, The Netherlands; and <sup>3</sup>Laboratory for Thrombosis Research, KU Leuven, Kortrijk, Belgium

## ABSTRACT

Initial platelet arrest at the exposed arterial vessel wall is mediated through glycoprotein Ib $\alpha$  binding to the A1 domain of von Willebrand factor. This interaction occurs at sites of elevated shear force, and strengthens upon increasing hydrodynamic drag. The increased interaction requires shear-dependent exposure of the von Willebrand factor A1 domain, but the contribution of glycoprotein Ib $\alpha$  remains ill defined. We have previously found that glycoprotein Ib $\alpha$  forms clusters upon platelet cooling and hypothesized that such a property enhances the interaction with von Willebrand factor under physiological conditions. We analyzed the distribution of glycoprotein Ib $\alpha$  with Förster resonance energy transfer using time-gated fluorescence lifetime imaging microscopy. Perfusion at a shear rate of 1,600 s<sup>-1</sup> induced glycoprotein Ib $\alpha$  clusters on platelets adhered to von Willebrand factor, while clustering did not require von Willebrand factor contact at 10,000 s<sup>-1</sup>. Shear-induced clustering was reversible, not accompanied by granule release or  $\alpha$ IIb $\beta$ 3 activation and improved glycoprotein Ib $\alpha$ -dependent platelet interaction with von Willebrand factor. Clustering required glycoprotein Ib $\alpha$  translocation to lipid rafts and critically depended on arachidonic acid-mediated binding of 14-3-3 $\zeta$  to its cytoplasmic tail. This newly identified mechanism emphasizes the ability of platelets to respond to mechanical force and provides new insights into how changes in hemodynamics influence arterial thrombus formation.

## Introduction

Platelet adhesion to subendothelial matrices in the damaged vessel wall is the prime event in the arrest of bleeding. Recruitment of platelets to sites of vascular injury is hampered by the rapid flow of blood in arteries and arterioles. In these vessels, the interaction between von Willebrand factor (VWF), a multimeric plasma glycoprotein, and the platelet glycoprotein (GP) Ib-IX-V receptor complex is critical for initial platelet adhesion.<sup>1</sup> This interaction requires unfolding of the VWF A1 domain and allows platelets to decelerate until they attach firmly in a process assisted by platelet integrins.<sup>1,2</sup> Defects in both the GPIb-IX-V complex (Bernard Soulier syndrome) and VWF (von Willebrand disease) result in a bleeding diathesis, which underscores the importance of this interaction in hemostasis.<sup>3,4</sup>

The GPIb-IX-V complex consists of four transmembrane subunits; GPIb $\alpha$ , GPIb $\beta$ , GPIX and GPV that are expressed in a 2:4:2:1 stoichiometry.<sup>5</sup> Each platelet contains approximately 25,000 copies of GPIb $\alpha$ , the subunit that binds to the VWF A1 domain.<sup>6</sup> The extracellular domain (residues 1-485) of GPIb $\alpha$  consists of an N-terminal flank, seven leucine-rich repeats, a C-terminal flank, a sulphated region and a highly glycosylated macroglycopeptide domain. Residues 486-514 form the transmembrane domain and the cytoplasmic tail consists of 96 amino acid residues (residues 515-610),<sup>7,9</sup> which contain binding sites for multiple intracellular proteins, including filamin A<sup>10</sup>

and the adaptor protein 14-3-3 $\zeta$ .<sup>11</sup> The region that interacts with the VWF A1 domain resides within the concave face of the leucine-rich repeat domain of GPIb $\alpha$ .<sup>12,13</sup> Despite the fundamental importance in initiating platelet adhesion, the molecular mechanism regulating the VWF-GPIb $\alpha$  interaction remains incompletely understood.

Binding of VWF to GPIb $\alpha$  requires the dynamic conditions of flowing blood. The unique biomechanical properties of VWF and GPIb $\alpha$  allow the interaction to strengthen upon increasing hemodynamic drag.<sup>14</sup> An explanation for this counterintuitive finding is that VWF needs to change its conformation to allow GPIb $\alpha$  access to the A1 domain. Elevated shear force and immobilization on a surface trigger this conformational change *in vivo*, a process mimicked by the antibiotic ristocetin *in vitro*.<sup>15</sup> The interaction between VWF and GPIb $\alpha$  is also regulated through changes in GPIb $\alpha$ . This molecule's adhesive properties depend on translocation to cholesterol-rich membrane domains known as lipid rafts,<sup>16,17</sup> which may increase the local density of GPIb $\alpha$  receptors and stimulate their signaling properties. Indeed, studies with Chinese hamster ovary cells in which GPIb $\alpha$  was artificially dimerized have suggested that receptor clustering increases the overall strength of the VWF-GPIb $\alpha$  interaction.<sup>18,19</sup>

During efforts to optimize the storage conditions of platelet concentrates used for transfusion, we recently demonstrated that GPIb $\alpha$  clusters in lipid rafts when platelets are kept at low temperature.<sup>20</sup> Analysis of Förster resonance energy transfer

©2013 Ferrata Storti Foundation. This is an open-access paper. doi:10.3324/haematol.2013.087221

The online version of this article has a Supplementary Appendix.

Manuscript received on March 1, 2013. Manuscript accepted on June 4, 2013.

Correspondence: r.t.urbanus@umcutrecht.nl

(FRET) by fluorescence lifetime imaging microscopy (FLIM) revealed that cooling of platelets triggers [GPIb $\alpha$ -GPIb $\alpha$ ] associations in lipid rafts within a range of 1-10 nm. In the present study, we assessed whether clustering of GPIb $\alpha$  occurs under physiological conditions, investigated its influence on VWF interaction and identified the responsible molecular mechanism.

## Methods

### The patient

Citrated blood (10.9 mM f.c.) was obtained from a patient with von Willebrand disease type 3. Permission was obtained from the local medical ethics committee. The patient had no detectable plasma VWF (<0.1%), 1% plasma factor VIII, <1% factor VIII activity, no ristocetin-induced platelet aggregation, and a normal platelet count and volume.<sup>21</sup>

### Materials, antibodies, platelet preparation and incubations

A detailed description of the materials, antibodies, platelet preparation and incubations used in this study can be found in the *Online Supplementary Methods*.

### Platelet adhesion and rolling under flow conditions

A parallel plate perfusion chamber<sup>22</sup> was used to investigate platelet adhesion and rolling. Further details are available in the *Online Supplementary Methods*.

### Exposure to shear force

Platelets were exposed to shear force by perfusion through a microcapillary (inner diameter 760  $\mu$ m, blocked with 4% bovine serum albumin). Washed platelets were resuspended in HT buffer (2.5x10<sup>11</sup> cells/L, pH 7.3) supplemented with 4% human albumin. Platelet suspensions were prewarmed to 37°C for 5 min and perfused through the microcapillary at indicated shear rates for 5 sec. The length of the microcapillaries was matched with the shear rate, which means that the platelet suspensions had similar shear exposure times at different shear rates. Indicated shear rates are the maximal shear rates to which platelets were exposed near the wall of the microcapillary. The wall shear rate ( $\gamma_w$ ) inside a microcapillary is described as

$$\text{wall shear rate } (\gamma_w) = \frac{4Q}{\pi r^3}$$

Where  $Q$  is the volumetric flow rate and  $r$  is the inner radius of the microcapillary.

### Agglutination

Platelet agglutination was measured in a Chrono-log Lumi-Aggregometer (model 700, Chrono-log Corporation, Haverton, PA, USA) with Aggrolink 8.0 software. Washed platelets in HT buffer were pre-incubated with the prostacyclin (PGI<sub>2</sub>) analog iloprost and dRGDW (5 min, 37°C) and stimulated with VWF (10  $\mu$ g/mL) and ristocetin (0.3 mg/mL) while stirring (900 rpm). Data are expressed as percentage of maximal agglutination, with light transmission through HT buffer set at 100%.

### Flow cytometric analysis, immunoprecipitations and western blots

A detailed description of the flow cytometric analysis, immunoprecipitations and western blots can be found in the *Online Supplementary Methods*.

### Analysis of GPIb $\alpha$ distribution by Förster resonance energy transfer and fluorescence lifetime imaging microscopy

GPIb $\alpha$  distribution was analyzed by FRET/FLIM as described elsewhere.<sup>20</sup> In brief, 6B4-Fab fragments conjugated to either Alexa Fluor-488 or Alexa Fluor-594 (6B4-488 and 6B4-594, respectively) were incubated with fixed platelet samples under conditions in which each Fab labeled ~50% of the total number of receptors. GPIb $\alpha$  translocation to lipid rafts was determined by labeling GPIb $\alpha$  with 6B4-488 and monosialo-tetrahexosylganglioside (GM1) with Cholera toxin subunit B conjugated to Alexa Fluor-594 (CTB-594; 5  $\mu$ g/mL). The fluorescence lifetimes of the donor fluorophore (6B4-488) were determined in the absence and presence of acceptor fluorophore (6B4-594 or CTB-594) and used to calculate the FRET efficiency, defined as

$$\text{FRET Efficiency} = \frac{\tau_D - \tau_{D/A}}{\tau_D} \times 100\%$$

where  $\tau$  is the donor fluorophore's lifetime in nanoseconds in the absence ( $\tau_D$ ) and presence ( $\tau_{D/A}$ ) of the acceptor fluorophore. To determine variation in FRET efficiency, the lifetimes of three randomly chosen quadrants were quantified.

### Statistical analysis

Data are means  $\pm$  SEM. Statistical analysis was based on GraphPad Prism 5 (San Diego, CA, USA). Differences between control platelets and incubations were analyzed by the Mann-Whitney test.  $P$ -values less than 0.05 (\* or \*\*) and between incubations (!-\*-!) were considered statistically significant.

## Results

### Platelet adhesion to von Willebrand factor under conditions of flow triggers GPIb $\alpha$ clustering

Platelet adhesion at shear rates above 1,000 s<sup>-1</sup> depends on the interaction between surface-bound VWF and GPIb $\alpha$ .<sup>1</sup> We analyzed the effect of this interaction on the spatial distribution of GPIb $\alpha$  on the platelet plasma membrane with FRET/FLIM. Whereas GPIb $\alpha$  molecules were dispersed in resting platelets (Figure 1A,B), indicated by a FRET efficiency of 0.9 $\pm$ 0.2%, GPIb $\alpha$  clustered upon adhesion to VWF (FRET efficiency 10.3 $\pm$ 0.9%). Clustering was not caused by close contact between adjacent platelets, as FRET efficiency did not differ between single platelets and platelets that adhered as small aggregates (*Online Supplementary Figure S1A,B*). As the platelet-VWF interaction is influenced by flow conditions, we analyzed the GPIb $\alpha$  distribution of platelets adhered to VWF at different shear rates. Adhesion to VWF at 300 s<sup>-1</sup> left GPIb $\alpha$  dispersed, but perfusion at 750 s<sup>-1</sup> and higher induced clustering (Figure 1C). The observed increase in clustering was not the result of more efficient adhesion, as the number of platelets binding to VWF was similar at each shear rate (*Online Supplementary Figure S1C*). To investigate whether changes in GPIb $\alpha$  distribution were specific for adhesion to VWF, platelets were perfused over collagen. Adhesion to collagen at a low shear rate (300 s<sup>-1</sup>) in the presence or absence of VWF resulted in FRET efficiencies similar to those observed in resting platelets (Figure 1D). Perfusion over collagen at 1,600 s<sup>-1</sup> in the absence of VWF had little effect on GPIb $\alpha$  distribution. In contrast, addition of VWF prior to perfusion at 1,600 s<sup>-1</sup> increased FRET efficiency to 8.3 $\pm$ 0.6%, indicating that clustering of GPIb $\alpha$  requires the presence of VWF.

### Exposure to high shear leads to reversible von Willebrand factor-independent GPIb $\alpha$ clustering

The change in GPIb $\alpha$  distribution measured on surface-attached platelets might be the result of shear, of rolling/attachment or both. To understand the contribution of shear, we perfused platelets in VWF-free buffer through a microcapillary tube at different shear rates in the absence of an adhesive surface. FRET/FLIM analysis showed that a shear rate of 300 s<sup>-1</sup> left GPIb $\alpha$  dispersed. Exposure to 1,600 s<sup>-1</sup> had a minor effect on GPIb $\alpha$  distribution, whereas a shear rate of 10,000 s<sup>-1</sup> increased FRET efficiency to 9.1±0.6% (Figure 2A). Addition of exogenous VWF prior to perfusion at a shear rate of 10,000 s<sup>-1</sup> did not further increase clustering. Platelet  $\alpha$ -granules also contain VWF,<sup>23</sup> which might be released during platelet isolation and thereby influence GPIb $\alpha$  clustering. To investigate this possibility, experiments were repeated using a nanobody against VWF which prevents its binding to GPIb $\alpha$ . Exposure of platelets to shear force in the presence of this nanobody led to the same increase in FRET efficiency as control platelets (Figure 2B). GPIb $\alpha$  clustering induced by a shear rate of 10,000 s<sup>-1</sup> was also similar in platelets from a patient with VWD type 3 (Online Supplementary Figure S2A), indicating that GPIb $\alpha$  clusters independently of the presence of VWF.

GPIb $\alpha$  clustering was reversible, as exposure to shear

followed by incubations under static conditions resulted in a gradual decline to the range found in resting platelets (Figure 2C). Platelet exposure to a shear rate of 10,000 s<sup>-1</sup> did not result in P-selectin expression,  $\alpha$ IIb $\beta$ 3 activation, VWF binding (Figure 2D), cytoskeleton reorganization or altered whole protein tyrosine phosphorylation (Online Supplementary Figure S2B,C). Conversely, clustering was not induced by stimulation with cross-linked collagen-related peptide (CRP), thrombin receptor activating peptide (TRAP) or the thromboxane A<sub>2</sub> receptor (TP $\alpha$ ) agonist U46619 under static conditions (Figure 2E). Ristocetin-induced VWF binding did induce clustering of GPIb $\alpha$ . Transient GPIb $\alpha$  clustering did not affect the ability of platelets to respond to agonists, because stimulation with TRAP or CRP before and after exposure to shear resulted in similar levels of P-selectin expression and  $\alpha$ IIb $\beta$ 3 activation (Figure 2F).

### Platelet interaction with von Willebrand factor is stimulated by clustered GPIb $\alpha$

To clarify whether changes in GPIb $\alpha$  distribution contributed to platelet responsiveness to VWF, agglutination was measured in platelets with shear-induced clustered GPIb $\alpha$ . VWF and a suboptimal concentration of ristocetin were used and aggregation was prevented by pre-incubation with iloprost, a stable analog of prostacyclin, and

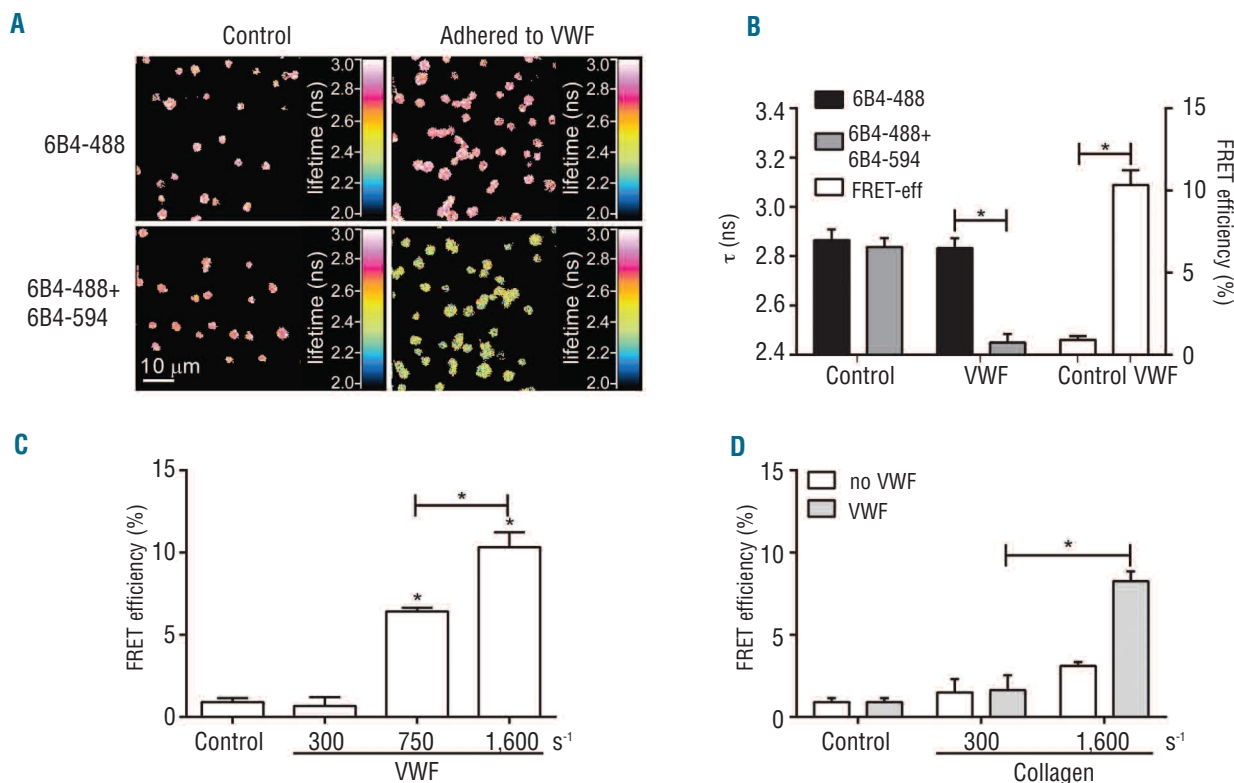


**Figure 1.** Platelet adhesion to VWF induces clustering of GPIb $\alpha$ . (A) Freshly isolated resting platelets (control; left panels) or platelets adhered to VWF after whole blood perfusion (1 min, 37 °C) at a shear rate of 1,600 s<sup>-1</sup> (right panels) were analyzed for GPIb $\alpha$  distribution by FRET/FLIM. Platelets were fixed with 2% paraformaldehyde and stained with 1  $\mu$ g/mL 6B4-488 (donor) in the absence (top panels) and presence of 1  $\mu$ g/mL 6B4-594 (acceptor; bottom panels). The fluorescence lifetimes in nanoseconds (ns) are shown in false color images. (B) Quantification of fluorescence lifetime values of donor probe in the absence and presence of acceptor probe of platelets treated under the conditions of (A). Corresponding FRET efficiencies are calculated as described in the Methods. (C-D) FRET/FLIM analysis of platelets adhered to VWF after whole blood perfusion (C) or to collagen after reconstituted blood perfusion (D) at indicated shear rates (1 min, 37 °C). Reconstituted blood over collagen was performed in the absence (open bars) and presence (gray bars) of 10  $\mu$ g/mL VWF (n=4).

dRGDW. Neither agent affected shear-induced GPIb $\alpha$  clustering (*data not shown*). Maximal agglutination of platelets with pre-clustered GPIb $\alpha$  was four-fold higher than with controls (Figure 3A,B).

VWF enables platelets to roll over the damaged vessel wall until they attach firmly in an integrin-dependent manner. The effect of GPIb $\alpha$  clustering was measured by platelet perfusion over a VWF-coated surface in the presence of dRGDW to block  $\alpha$ IIb $\beta$ 3-mediated attachment. Induction of GPIb $\alpha$  clustering prior to perfusion reduced the rolling velocity by 40% (Figure 3C,D). These data show that GPIb $\alpha$  clustering facilitates the platelet-VWF interaction.

### GPIb $\alpha$ translocates to lipid rafts and forms clusters through 14-3-3 $\zeta$ binding

Platelet binding to VWF depends on reallocation of GPIb $\alpha$  in membrane domains enriched in sphingomyelin and cholesterol, known as lipid rafts.<sup>16,17</sup> To understand the role of raft allocation in GPIb $\alpha$  clustering, GPIb $\alpha$  was labeled with 6B4-488 (donor) and the raft marker GM1 with CTB conjugated to Alexa Fluor-594 (CTB-594; acceptor). The surface of resting platelets showed little co-localization but adhesion to VWF or exposure to high shear (10,000 s<sup>-1</sup>) induced GPIb $\alpha$ -GPIb $\alpha$  as well as GPIb $\alpha$ -GM1 associations, suggesting that clustering and raft translocation go hand in hand (Figure 4A). Disruption of lipid rafts by cholesterol depletion with methyl- $\beta$ -cyclodextrin (m $\beta$ CD) effectively abrogated GPIb $\alpha$  clustering. The time-

dependent decay of shear-induced GPIb $\alpha$  clusters closely followed raft translocation, again suggesting a tight inter-relationship (Figure 4B).

Binding of the adaptor protein 14-3-3 $\zeta$  to the cytoplasmic tail of GPIb $\alpha$  is essential for platelet interaction with VWF.<sup>24,25</sup> To assess the role of 14-3-3 $\zeta$  in GPIb $\alpha$  clustering, we pre-incubated platelets with MP $\alpha$ C. This membrane permeable peptide represents the critical 14-3-3 $\zeta$  binding site on GPIb $\alpha$ , which includes the constitutively phosphorylated Ser-609 residue on its cytoplasmic tail.<sup>24,26,27</sup> As expected, the peptide prevented VWF-induced 14-3-3 $\zeta$  binding to GPIb $\alpha$  (Online Supplementary Figure S2). Figure 4C shows that pre-incubation with MP $\alpha$ C had little effect on lipid raft translocation induced by platelet adhesion to VWF, but completely abrogated clustering of GPIb $\alpha$ . Control peptide M $\alpha$ C, which lacks phosphorylation at Ser-609, had no effect on GPIb $\alpha$  redistribution. FRET/FLIM analysis of platelets exposed to a shear rate of 10,000 s<sup>-1</sup> procured similar results (Figure 4D), demonstrating that 14-3-3 $\zeta$  binding to the cytoplasmic tail of GPIb $\alpha$  is essential for its clustering. To elucidate the importance of 14-3-3 $\zeta$ -induced clustering, we determined the rolling velocity of platelets perfused over VWF in the presence of MP $\alpha$ C (Figure 4E). While control peptide M $\alpha$ C had no effect, the rolling velocity of platelets pre-incubated with MP $\alpha$ C increased more than two-fold. Moreover, inhibition of 14-3-3 $\zeta$ -induced GPIb $\alpha$  clustering impaired stable adhesion to VWF during whole blood perfusion (Figure 4F).

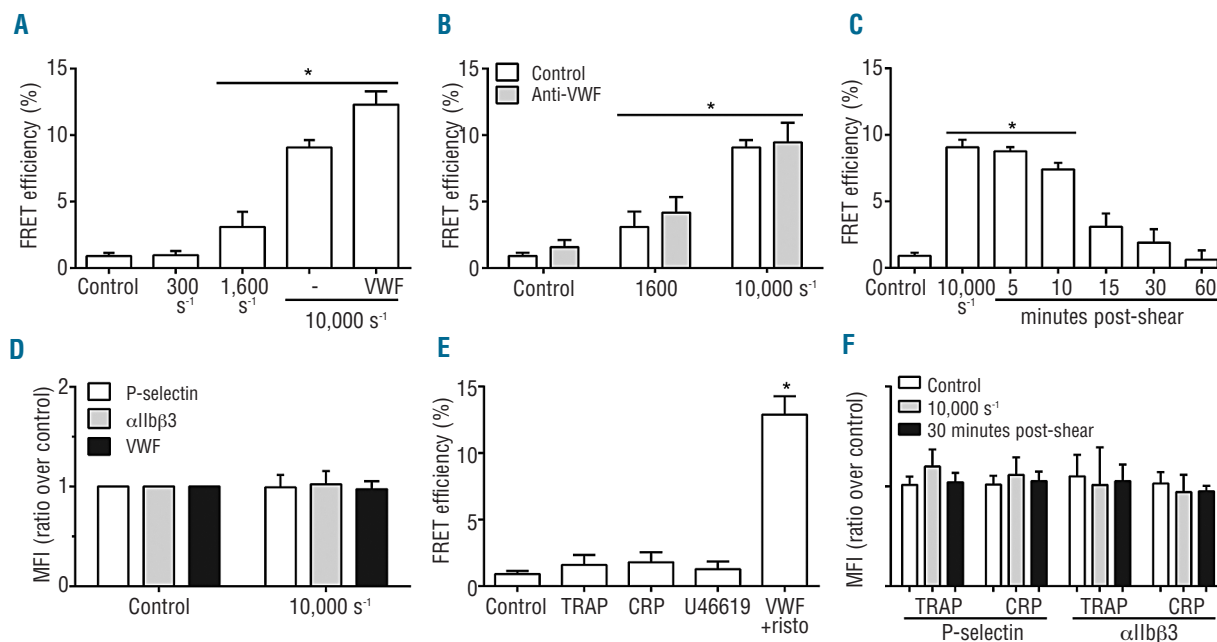


**Figure 2.** High shear force induces reversible GPIb $\alpha$  clustering in the absence of VWF. (A) Platelets resuspended in HT buffer (pH 7.3) supplemented with 4% albumin were exposed to indicated shear rates in the absence or presence of VWF (10  $\mu$ g/mL) by perfusion (37  $^{\circ}$ C) through a microcapillary tube for 5 s and analyzed for GPIb $\alpha$  distribution by FRET/FLIM. (B) Shear-induced GPIb $\alpha$  clustering occurs in the absence of VWF. Platelets in the absence or presence of a nanobody against VWF (10  $\mu$ g/mL) that prevents its interaction with GPIb $\alpha$  were exposed to indicated shear rates and analyzed by FRET/FLIM. (C) Shear-induced GPIb $\alpha$  clustering is reversible. Platelets exposed to 10,000 s<sup>-1</sup> were monitored for clustering at indicated time intervals post-shear, which after 10 min decreased to control levels. (D) Platelets were analyzed by FACS for expression of P-selectin,  $\alpha$ IIb $\beta$ 3 activation and VWF binding after exposure to shear. (E) FRET/FLIM analysis of platelets stimulated by CRP (1  $\mu$ g/mL), TRAP-6 (20  $\mu$ M), U46619 (10  $\mu$ M) or ristocetin (0.3 mg/mL) and VWF (10  $\mu$ g/mL) for 5 min at 37  $^{\circ}$ C in the absence of shear. (F) The effects of reversible GPIb $\alpha$  clustering on platelet responsiveness were analyzed by stimulating platelets with TRAP or CRP 0 and 30 min post-shear. FACS analysis revealed that agonist-induced surface expression of P-selectin or  $\alpha$ IIb $\beta$ 3 activation was similar to that of control platelets. Data are presented as the ratio of mean fluorescence intensity (MFI) of treated platelets over control platelets (n=4).



### Arachidonic acid mediates 14-3-3 $\zeta$ -induced GPIb $\alpha$ clustering

Platelet interaction with VWF or incubation at low temperature activates the stress kinase P38-mitogen-activated protein kinase (P38MAPK), which liberates arachidonic acid (AA) from membrane phospholipids through cytosolic phospholipase A<sub>2</sub>.<sup>20,28,29</sup> Incubation with inhibitors at 37°C indicated that P38MAPK-mediated AA release might support GPIb $\alpha$ -GPIb $\alpha$  interactions during exposure to shear. The P38MAPK inhibitor SB203580 and the cytosolic phospholipase A<sub>2</sub> inhibitor AACOCF<sub>3</sub> inhibited the rise in FRET efficiency induced by high shear. The low FRET efficiency observed under static conditions increased 12-fold upon addition of AA. The intracellular accumulation of free AA might therefore contribute to GPIb $\alpha$  clustering (Figure 5A). The FRET efficiency of shear-treated platelets decreased upon subsequent incubations under static conditions (Figure 2C).

In platelets, liberated AA is metabolized by cyclo-oxygenase-1 and lipo-oxygenase to thromboxane A<sub>2</sub> and other eicosanoids, which could account for the reversibility of shear-induced GPIb $\alpha$  clustering. Indeed, accumulation of AA by inhibition of these enzymes with indomethacin and 5,8,11-eicosatriynoic acid prevented GPIb $\alpha$  clusters from dispersing after exposure to high shear (Figure 5B). AA release triggered by platelet stimulation with CRP or TRAP in the presence of indomethacin and 5,8,11-eicosatriynoic acid also induced clustering of GPIb $\alpha$  (Figure 5C). Control studies confirmed that SB203580 blocked shear-induced P38MAPK phosphorylation/activation whereas the other treatments left the enzyme undisturbed (Figure 5D). Treatments that inhibited AA release prevented shear-induced 14-3-3 $\zeta$ -GPIb $\alpha$  association and blockade of AA degradation and the separate addition of AA preserved the complex (Figure 5E). These data indicate that liberated AA binds 14-3-3 $\zeta$  and facilitates its translo-

cation to the cytoplasmic tail of GPIb $\alpha$ .<sup>20,28</sup>

The inhibitors of AA release and degradation affected platelet rolling velocity over a VWF surface. Inhibition of AA release induced by shear increased the rolling velocity, whereas treatments that preserved accumulation of AA resulted in reduced velocities (Figure 5F). These data indicate that the AA-mediated transfer of 14-3-3 $\zeta$  to the GPIb $\alpha$  cytoplasmic tail induces GPIb $\alpha$  clustering which supports platelet interaction with VWF at high shear.

### Discussion

Our results demonstrate that the exposure of platelets to high shear leads to clustering of GPIb $\alpha$  and enhances the interaction with VWF. Shear-induced clustering is reversible and not associated with granule release or activation of  $\alpha$ IIb $\beta$ 3. Clustering requires lipid raft translocation and critically depends on AA-mediated 14-3-3 $\zeta$  binding to the cytoplasmic tail of GPIb $\alpha$  (Figure 6).

Previous studies found a role for receptor clustering in the GPIb $\alpha$ -VWF interaction.<sup>18,19</sup> Experiments with Chinese hamster ovary cells showed that intracellular dimerization of a modified GPIb $\alpha$  construct increases the overall bond strength with VWF. We found that GPIb $\alpha$  formed clusters in platelets adhered to VWF after perfusion at a shear rate of 750 s<sup>-1</sup> or higher. At these shear rates, platelet adhesion strongly depends on the interaction between GPIb $\alpha$  and VWF, because only this interaction is sufficiently fast and strong to withstand the associated hemodynamic drag.<sup>1</sup> Our results indicate that GPIb $\alpha$  clustering contributes to GPIb $\alpha$ -mediated platelet adhesion to VWF, as inhibition of clustering strongly attenuated both platelet rolling velocity and adhesion.

Initial adhesion to VWF increases the hemodynamic drag on platelets substantially and results in the formation

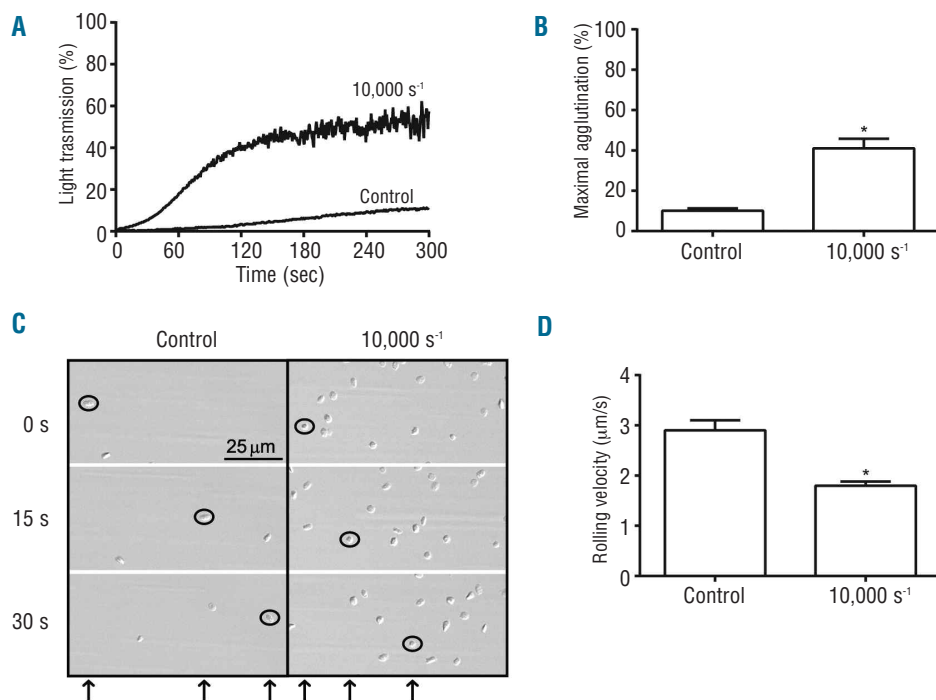


**Figure 3.** GPIb $\alpha$  clustering improves platelet interaction with VWF. Resting platelets (control) or platelets exposed to 10,000 s<sup>-1</sup> were pre-incubated with dRGDW and iloprost for 5 min at 37°C. Platelet agglutination and rolling velocity experiments were performed immediately after shear exposure. (A-B) Platelets were stimulated with suboptimal concentrations of ristocetin (0.3 mg/mL) and VWF (10 μg/mL) and agglutination (A) was measured at 37°C while stirring. (B) Quantification of mean maximal agglutination (n=3). (C-D) Analysis of platelet rolling velocity over VWF at a shear rate of 1,600 s<sup>-1</sup>. (C) Single platelets (black circles) were tracked over distance in time from which the rolling velocity was determined. Black arrows indicate the location of a single platelet at 0, 15 and 30 s. (D) Quantification of rolling velocity in μm/s. Rolling velocity was significantly reduced after pre-exposure to a shear rate of 10,000 s<sup>-1</sup> (n=5).

of membrane tethers that are pulled from the cell surface.<sup>30,31</sup> Upon adhesion to VWF, clustering was observed at a shear rate of 750 s<sup>-1</sup> or higher. In the absence of an adhesive surface, GPIb $\alpha$  clustering required exposure to 10,000 s<sup>-1</sup>, a shear rate found in stenotic arteries. By definition, only those platelets nearest to the vessel wall are subjected to this shear rate. Shear exposure is, therefore, probably limited to part of the platelet population perfused through a microcapillary. Nevertheless, this short exposure to shear stress induced clustering of GPIb $\alpha$ , illustrating the high sensitivity of platelets to mechanical stress. The combined force of shear exposure and tensile stress exerted on GPIb $\alpha$  when bound to VWF apparently cooperate in facilitating GPIb $\alpha$  clustering. Shear-induced clustering did not coincide with platelet activation, which is in line with earlier reports of VWF-dependent adhesion<sup>32</sup> or aggregation of discoid platelets<sup>33</sup> at high shear rates.

The effects of clustering on the interaction with VWF probably reflect avidity modulation, where an increased local density of GPIb $\alpha$  molecules increases the number of ligand-receptor bonds. Based on crystal structure studies, it is less likely that GPIb $\alpha$  clustering facilitates binding of two GPIb $\alpha$  molecules to a single A1 domain.<sup>12,34</sup> Under the influence of elevated hemodynamic drag, VWF-bound GPIb $\alpha$  can subsequently undergo a conformational change

that further strengthens the interaction.<sup>14</sup>

Disruption of lipid rafts by cholesterol depletion strongly impairs platelet adhesion to VWF under conditions of flow, indicating that GPIb $\alpha$  localization to these regions is essential for its function.<sup>16</sup> Lipid rafts are viewed as platforms that can physically concentrate receptors, adaptor proteins and effector enzymes, which lead to amplification of signaling events. We observed little GPIb $\alpha$  localization in rafts on the surface of resting platelets, which increased about three-fold upon ligation to immobilized VWF or exposure to high shear in solution. Disruption of rafts prevented GPIb $\alpha$  from clustering. Although translocation was essential for this process, clustering depended critically on the interaction between 14-3-3 $\zeta$  and GPIb $\alpha$ . The importance of the [14-3-3 $\zeta$ -GPIb $\alpha$ ] association for the interaction of platelets with VWF is well established,<sup>24,25</sup> but the exact mode of action remains poorly defined. It has been suggested that this association participates in  $\alpha$ IIb $\beta$ 3 integrin activation in GPIb-IX-expressing Chinese hamster ovary cells.<sup>35,36</sup> We show that inhibition of 14-3-3 $\zeta$  binding to GPIb $\alpha$  impaired adhesion to VWF and increased rolling velocity. The presence of iloprost and dRGDW excluded involvement of  $\alpha$ IIb $\beta$ 3 integrin in platelet rolling on VWF. Together, these data indicate that the 14-3-3 $\zeta$  association with GPIb $\alpha$  directly improves

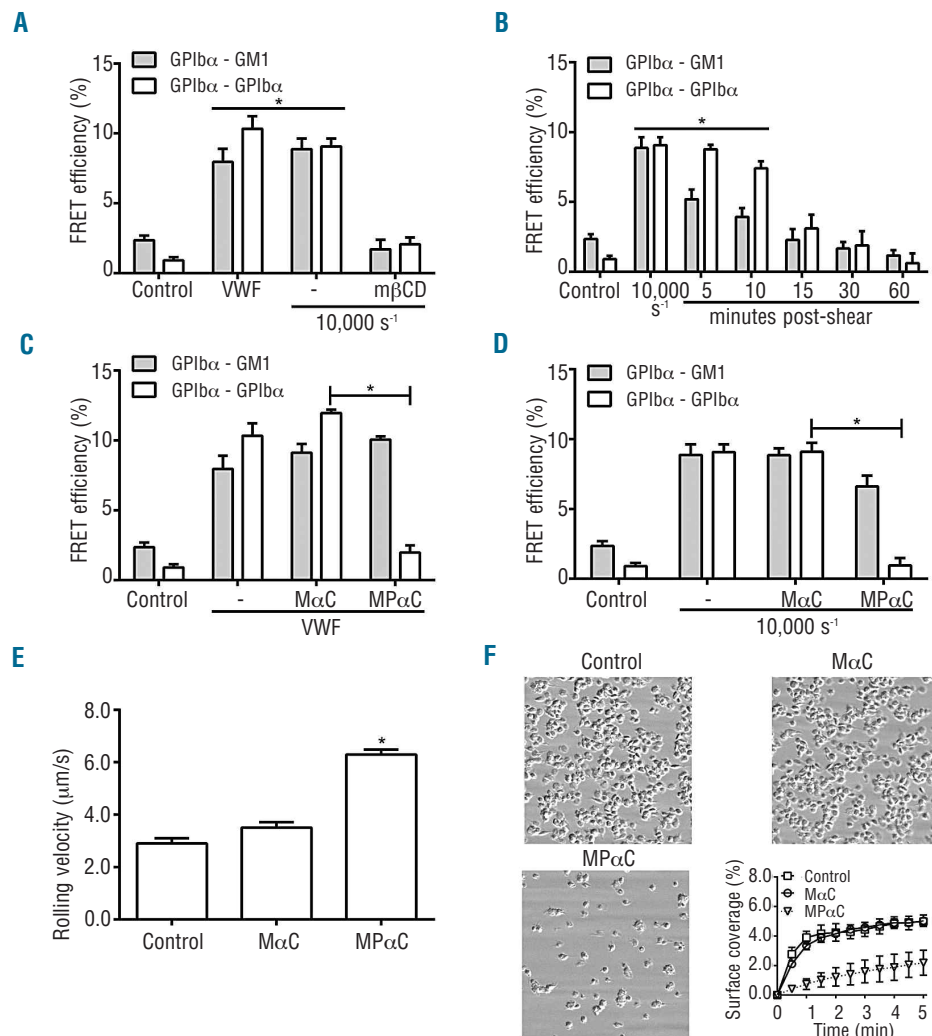


**Figure 4.** Clustering of GPIb $\alpha$  requires translocation to lipid rafts and 14-3-3 $\zeta$  binding to its cytoplasmic tail. GPIb $\alpha$  translocation to lipid rafts was measured by labeling GPIb $\alpha$  with 6B4-488 (donor, 1  $\mu$ g/mL) and raft-specific GM1 ganglioside with CTB-594 (acceptor; 5  $\mu$ g/mL). (A-D) FRET/FLIM analysis of [GPIb $\alpha$ -GM1] and [GPIb $\alpha$ -GPIb $\alpha$ ] associations. (A) GPIb $\alpha$  distribution of platelets adhered to VWF by whole blood perfusion at 1,600 s<sup>-1</sup> (VWF) or washed platelets perfused through a microcapillary at 10,000 s<sup>-1</sup>. Disruption of lipid rafts by cholesterol depletion with m $\beta$ CD (10 mM, 30 min at 37°C) prior to perfusion prevented changes in GPIb $\alpha$  distribution. (B) GPIb $\alpha$  translocation to lipid rafts induced by shear force is reversible after 10 min. (C-D) GPIb $\alpha$  clustering requires 14-3-3 $\zeta$  binding to its cytoplasmic tail. Binding of 14-3-3 $\zeta$  to GPIb $\alpha$  was prevented by pre-incubation with the cell-permeable peptide MP $\alpha$ C (100  $\mu$ M, 5 min at 37°C). FRET/FLIM analysis of platelets bound to VWF by perfusion (C) or exposed to shear (D) in the presence of control peptide M $\alpha$ C or MP $\alpha$ C. (E-F) Platelet interaction with VWF is impaired by prevention of 14-3-3 $\zeta$  binding to GPIb $\alpha$ . Analysis of platelet rolling velocity over VWF at 1,600 s<sup>-1</sup> (E) and quantification of platelet surface coverage during whole blood perfusion (F) in the presence of M $\alpha$ C or MP $\alpha$ C. (F) Snapshots were taken after 5 min of perfusion (n=4).

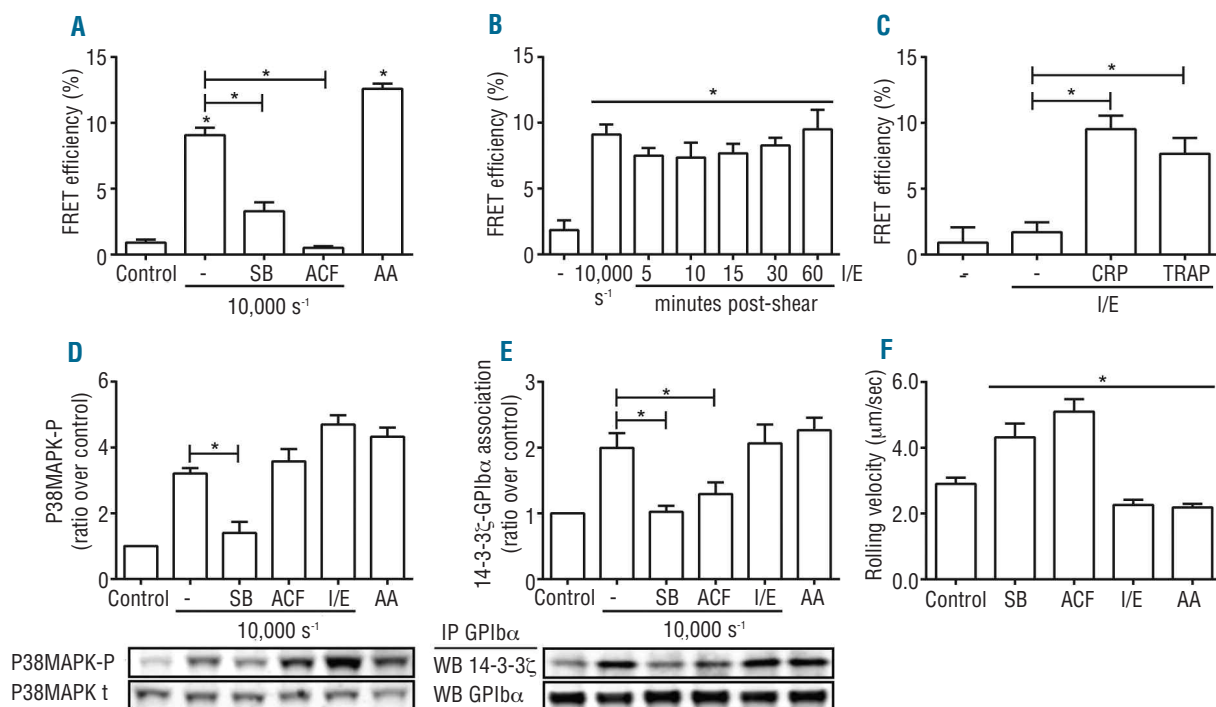


**Figure 5.** Binding of 14-3-3 $\zeta$  to GPIb $\alpha$  is regulated by AA. (A) Clustering of GPIb $\alpha$  is prevented by inhibitors of upstream regulators of intracellular AA release. Pre-incubation (10 min at 37°C) with P38MAPK inhibitor SB203580 (SB; 10  $\mu$ M) or cytosolic phospholipase A<sub>2</sub> inhibitor AACOCF<sub>3</sub> (ACF; 20  $\mu$ M) abolished shear-induced clustering of GPIb $\alpha$ . Platelet incubation with 10  $\mu$ M AA (5 min at 37°C) in the presence of TP $\alpha$  antagonist SQ30741 (25  $\mu$ M) induced GPIb $\alpha$  clustering. (B) Shear-induced clustering of GPIb $\alpha$  is maintained in the presence of inhibitors of AA metabolism. Inhibitors were against cyclooxygenase-1 (indomethacin; 30  $\mu$ M) and lipo-oxygenase (5, 8, 11-eicosatriynoic acid, ETI; 25  $\mu$ M), abbreviated as I/E. (C) Platelet stimulation with CRP or TRAP in the presence of indomethacin and ETI induces clustering of GPIb $\alpha$ . (D-E) Analysis of shear-induced phosphorylation of P38MAPK (D) and [14-3-3 $\zeta$ -GPIb $\alpha$ ] complex formation (E) under conditions described for (A) and (B). (F) Platelet rolling velocity increases in the presence of SB203580 and AACOCF<sub>3</sub> and is reduced in the presence of AA metabolism inhibitors (I/E) or exogenous AA, under conditions described for (A) and (B) (n=4).

platelet interaction with VWF by allowing receptor clustering. The dimeric nature of 14-3-3 $\zeta$  supports this finding.<sup>37</sup> Indeed, a similar mechanism has been described in muscle cells, in which clustering of the acetylcholine receptor depends on 14-3-3 $\zeta$ .<sup>38</sup>

P38MAPK is a kinase that is responsive to stress stimuli, including alterations in thermal<sup>28</sup> and shear conditions.<sup>39</sup> We found that platelet exposure to shear in solution leads to P38MAPK phosphorylation. Phosphorylated P38MAPK subsequently activates cytosolic phospholipase A<sub>2</sub> to release AA from membrane phospholipids.<sup>40</sup> Our study reveals a central role for AA in GPIb $\alpha$  clustering. Inhibition of AA release during exposure to shear prevented the transfer of 14-3-3 $\zeta$  to the cytoplasmic tail of GPIb $\alpha$ . Moreover, addition of AA enhanced clustering and inhibition of AA metabolism resulted in irreversible clustering. The findings that AA binding to 14-3-3 $\zeta$  induces 14-3-3 $\zeta$  multimerization<sup>41</sup> and that AA-bound 14-3-3 $\zeta$  directly associates with GPIb $\alpha$ ,<sup>28</sup> both support the concept that the adaptor protein provides a platform for GPIb $\alpha$  clustering. In addition, lipid rafts are enriched in AA,<sup>42</sup> which may explain the dependence of GPIb $\alpha$  cluster formation on these membrane domains. Rolling experiments established the importance of AA-mediated GPIb $\alpha$  clustering, as inhibitors of AA release reduced platelet interaction with VWF, while its accumulation enhanced this initial step in adhesion.

Aspirin, a widely used antithrombotic drug, also interferes with AA conversion by inhibiting COX-1 activity. Our studies suggest that the use of aspirin may prolong

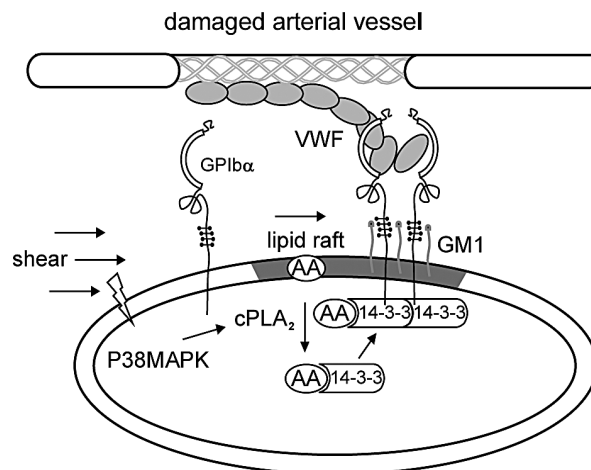


**Figure 6.** Schematic representation of initial platelet adhesion to VWF at the damaged arterial vessel wall. Shear triggers GPIb $\alpha$  translocation to lipid rafts and activates P38MAPK. This stress kinase subsequently activates cytosolic phospholipase A<sub>2</sub> (cPLA<sub>2</sub>), which liberates AA from membrane phospholipids. GPIb $\alpha$  clusters upon AA-mediated 14-3-3 $\zeta$  binding to its cytoplasmic tail, leading to enhanced interaction with VWF.

the presence of GPIb $\alpha$  clusters, which contradicts the antithrombotic effects of this drug. However, the inhibitory effects of aspirin are attributed to inhibition of thromboxane A<sub>2</sub>-enhanced platelet activation,<sup>43</sup> which is important for more advanced steps in thrombus forma-



tion. Interestingly, several studies have demonstrated that GPIIb/IIIa-dependent platelet adhesion actually increases upon aspirin intake.<sup>44,45</sup> These unexplained findings may be the result of aspirin-enhanced GPIIb/IIIa clustering.

In conclusion, we have defined a central role for GPIIb/IIIa clustering in platelet interaction with VWF under conditions of flow. Clustering of GPIIb/IIIa requires translocation to lipid rafts and AA-mediated 14-3-3 $\zeta$  binding to its cytoplasmic tail. These findings illustrate the mechanosensitive properties of platelets and give a new perspective on the molecular mechanism of arterial thrombus formation.

### Acknowledgments

This study was supported by a grant from the Landsteiner Foundation of Blood Transfusion Research (LSBR grant n. 0807). Prof. Dr. JWN Akkerman is supported by the Netherlands Thrombosis Foundation. Dr. RT Urbanus is a research fellow of the Dutch Heart Foundation (grant n. 2010T068).

### Authorship and Disclosures

Information on authorship, contributions, and financial & other disclosures was provided by the authors and is available with the online version of this article at [www.haematologica.org](http://www.haematologica.org).

## References

- Savage B, Saldivar E, Ruggeri ZM. Initiation of platelet adhesion by arrest onto fibrinogen or translocation on von Willebrand factor. *Cell*. 1996;84(2):289-97.
- Schneider SW, Nuschele S, Wixforth A, Gorzelanny C, exander-Katz A, Netz RR, et al. Shear-induced unfolding triggers adhesion of von Willebrand factor fibers. *Proc Natl Acad Sci USA*. 2007;104(19):7899-903.
- Li C, Martin SE, Roth GJ. The genetic defect in two well-studied cases of Bernard-Soulier syndrome: a point mutation in the fifth leucine-rich repeat of platelet glycoprotein Ib alpha. *Blood*. 1995;86(10):3805-14.
- Weiss HJ, Rogers J, Brand H. Defective ristocetin-induced platelet aggregation in von Willebrand's disease and its correction by factor VIII. *J Clin Invest*. 1973;52(11):2697-707.
- Luo SZ, Mo X, Afshar-Kharghan V, Srinivasan S, Lopez JA, Li R. Glycoprotein Ibalpha forms disulfide bonds with 2 glycoprotein Ibbeta subunits in the resting platelet. *Blood*. 2007;109(2):603-9.
- Du X, Beutler L, Ruan C, Castaldi PA, Berndt MC. Glycoprotein Ib and glycoprotein IX are fully complexed in the intact platelet membrane. *Blood*. 1987;69(5):1524-7.
- Dong JF, Li CO, Lopez JA. Tyrosine sulfation of the glycoprotein Ib-IX complex: identification of sulfated residues and effect on ligand binding. *Biochemistry*. 1994;33(46):13946-53.
- Lopez JA, Chung DW, Fujikawa K, Hagen FS, Papayannopoulou T, Roth GJ. Cloning of the alpha chain of human platelet glycoprotein Ib: a transmembrane protein with homology to leucine-rich alpha 2-glycoprotein. *Proc Natl Acad Sci USA*. 1987;84(16):5615-9.
- Korrel SA, Clemetson KJ, Van HH, Kamerling JP, Sixma JJ, Vliegthart JF. Structural studies on the O-linked carbohydrate chains of human platelet glyocalicin. *Eur J Biochem*. 1984;140(3):571-6.
- Andrews RK, Fox JE. Identification of a region in the cytoplasmic domain of the platelet membrane glycoprotein Ib-IX complex that binds to purified actin-binding protein. *J Biol Chem*. 1992;267(26):18605-11.
- Du X, Harris SJ, Tetaz TJ, Ginsberg MH, Berndt MC. Association of a phospholipase A2 (14-3-3 protein) with the platelet glycoprotein Ib-IX complex. *J Biol Chem*. 1994;269(28):18287-90.
- Huizinga EG, Tsuji S, Romijn RA, Schiphorst ME, de Groot PG, Sixma JJ, et al. Structures of glycoprotein Ibalpha and its complex with von Willebrand factor A1 domain. *Science*. 2002;297(5584):1176-9.
- Dumas JJ, Kumar R, McDonagh T, Sullivan F, Stahl ML, Somers WS, et al. Crystal structure of the wild-type von Willebrand factor A1-glycoprotein Ibalpha complex reveals conformation differences with a complex bearing von Willebrand disease mutations. *J Biol Chem*. 2004;279(22):23327-34.
- Kim J, Zhang CZ, Zhang X, Springer TA. A mechanically stabilized receptor-ligand flex-bond important in the vasculature. *Nature*. 2010;466(7309):992-5.
- Dong JF, Berndt MC, Schade A, McIntire LV, Andrews RK, Lopez JA. Ristocetin-dependent, but not botrocetin-dependent, binding of von Willebrand factor to the platelet glycoprotein Ib-IX-V complex correlates with shear-dependent interactions. *Blood*. 2001;97(1):162-8.
- Shrimpton CN, Borthakur G, Larrucea S, Cruz MA, Dong JF, Lopez JA. Localization of the adhesion receptor glycoprotein Ib-IX-V complex to lipid rafts is required for platelet adhesion and activation. *J Exp Med*. 2002;196(8):1057-66.
- Geng H, Xu G, Ran Y, Lopez JA, Peng Y. Platelet glycoprotein Ib beta/IX mediates glycoprotein Ib alpha localization to membrane lipid domain critical for von Willebrand factor interaction at high shear. *J Biol Chem*. 2011;286(24):21315-23.
- Kasirer-Friede A, Ware J, Leng L, Marchese P, Ruggeri ZM, Shattil SJ. Lateral clustering of platelet GP Ib-IX complexes leads to up-regulation of the adhesive function of integrin alpha IIb beta 3. *J Biol Chem*. 2002;277(14):11949-56.
- Arya M, Lopez JA, Romo GM, Cruz MA, Kasirer-Friede A, Shattil SJ, et al. Glycoprotein Ib-IX-mediated activation of integrin alpha(IIb)beta(3): effects of receptor clustering and von Willebrand factor adhesion. *J Thromb Haemost*. 2003;1(6):1150-7.
- Gitz E, Koekman CA, van den Heuvel DJ, Deckmyn H, Akkerman JW, Gerritsen HC, et al. Improved platelet survival after cold storage by prevention of glycoprotein Ibalpha clustering in lipid rafts. *Haematologica*. 2012;97(12):1873-81.
- Nichols WL, Hultin MB, James AH, Manco-Johnson MJ, Montgomery RR, Ortel TL, et al. von Willebrand disease (VWD): evidence-based diagnosis and management guidelines, the National Heart, Lung, and Blood Institute (NHLBI) Expert Panel report (USA). *Haemophilia*. 2008;14(2):171-232.
- Sakariassen KS, Aarts PA, de Groot PG, Houdijk WP, Sixma JJ. A perfusion chamber developed to investigate platelet interaction in flowing blood with human vessel wall cells, their extracellular matrix, and purified components. *J Lab Clin Med*. 1983;102(4):522-35.
- Wencel-Drake JD, Painter RG, Zimmerman TS, Ginsberg MH. Ultrastructural localization of human platelet thrombospondin, fibrinogen, fibronectin, and von Willebrand factor in frozen thin section. *Blood*. 1985;65(4):929-38.
- Dai K, Bodnar R, Berndt MC, Du X. A critical role for 14-3-3zeta protein in regulating the VWF binding function of platelet glycoprotein Ib-IX and its therapeutic implications. *Blood*. 2005;106(6):1975-81.
- Yuan Y, Zhang W, Yan R, Liao Y, Zhao L, Ruan C, et al. Identification of a novel 14-3-3zeta binding site within the cytoplasmic domain of platelet glycoprotein Ibalpha that plays a key role in regulating the von Willebrand factor binding function of glycoprotein Ib-IX. *Circ Res*. 2009;105(12):1177-85.
- Bodnar RJ, Gu M, Li Z, Englund GD, Du X. The cytoplasmic domain of the platelet glycoprotein Ibalpha is phosphorylated at serine 609. *J Biol Chem*. 1999;274(47):33474-9.
- Du X, Fox JE, Pei S. Identification of a binding sequence for the 14-3-3 protein within the cytoplasmic domain of the adhesion receptor, platelet glycoprotein Ib alpha. *J Biol Chem*. 1996;271(13):7362-7.
- van der Wal DE, Gitz E, Du VX, Lo KS, Koekman CA, Versteeg S, et al. Arachidonic acid depletion extends survival of cold-stored platelets by interfering with the [glycoprotein Ibalpha - 14-3-3zeta] association. *Haematologica*. 2012;97(10):1514-22.
- Kramer RM, Roberts EF, Um SL, Borsch-Haubold AG, Watson SP, Fisher MJ, et al. p38 mitogen-activated protein kinase phosphorylates cytosolic phospholipase A2 (cPLA2) in thrombin-stimulated platelets. Evidence that proline-directed phosphorylation is not required for mobilization of arachidonic acid by cPLA2. *J Biol Chem*. 1996;271(44):27723-9.
- Dopheide SM, Maxwell MJ, Jackson SP. Shear-dependent tether formation during platelet translocation on von Willebrand factor. *Blood*. 2002;99(1):159-67.
- Reininger AJ, Heijnen HF, Schumann H, Specht HM, Schramm W, Ruggeri ZM. Mechanism of platelet adhesion to von Willebrand factor and microparticle formation under high shear stress. *Blood*. 2006;107(9):3537-45.
- Ruggeri ZM, Orje JN, Habermann R, Federici AB, Reininger AJ. Activation-inde-



- pendent platelet adhesion and aggregation under elevated shear stress. *Blood*. 2006;108(6):1903-10.
33. Nesbitt WS, Westein E, Tovar-Lopez FJ, Tolouei E, Mitchell A, Fu J, et al. A shear gradient-dependent platelet aggregation mechanism drives thrombus formation. *Nat Med*. 2009;15(6):665-73.
  34. Uff S, Clemetson JM, Harrison T, Clemetson KJ, Emsley J. Crystal structure of the platelet glycoprotein Ib(alpha) N-terminal domain reveals an unmasking mechanism for receptor activation. *J Biol Chem*. 2002;277(38):35657-63.
  35. Gu M, Xi X, Englund GD, Berndt MC, Du X. Analysis of the roles of 14-3-3 in the platelet glycoprotein Ib-IX-mediated activation of integrin alpha(IIb)beta(3) using a reconstituted mammalian cell expression model. *J Cell Biol*. 1999;147(5):1085-96.
  36. Mangin P, David T, Lavaud V, Cranmer SL, Pikovski I, Jackson SP, et al. Identification of a novel 14-3-3zeta binding site within the cytoplasmic tail of platelet glycoprotein Ib(alpha). *Blood*. 2004;104(2):420-7.
  37. Fu H, Subramanian RR, Masters SC. 14-3-3 proteins: structure, function, and regulation. *Annu Rev Pharmacol Toxicol*. 2000;40:617-47.
  38. Lee CW, Han J, Bamberg JR, Han L, Lynn R, Zheng JQ. Regulation of acetylcholine receptor clustering by ADF/cofilin-directed vesicular trafficking. *Nat Neurosci*. 2009;12(7):848-56.
  39. Sumpio BE, Yun S, Cordova AC, Haga M, Zhang J, Koh Y, et al. MAPKs (ERK1/2, p38) and AKT can be phosphorylated by shear stress independently of platelet endothelial cell adhesion molecule-1 (CD31) in vascular endothelial cells. *J Biol Chem*. 2005;280(12):11185-91.
  40. Canobbio I, Reineri S, Sinigaglia F, Balduini C, Torti M. A role for p38 MAP kinase in platelet activation by von Willebrand factor. *Thromb Haemost*. 2004;91(1):102-10.
  41. Brock TG. Arachidonic acid binds 14-3-3zeta, releases 14-3-3zeta from phosphorylated BAD and induces aggregation of 14-3-3zeta. *Neurochem Res*. 2008;33(5):801-7.
  42. Pike LJ, Han X, Chung KN, Gross RW. Lipid rafts are enriched in arachidonic acid and plasmenylethanolamine and their composition is independent of caveolin-1 expression: a quantitative electrospray ionization/mass spectrometric analysis. *Biochemistry*. 2002;41(6):2075-88.
  43. Patrono C, Garcia Rodriguez LA, Landolfi R, Baigent C. Low-dose aspirin for the prevention of atherothrombosis. *N Engl J Med*. 2005;353(22):2373-83.
  44. Turner NA, Moake JL, Kamat SC, Schafer AI, Kleiman NS, Jordan R, et al. Comparative real-time effects on platelet adhesion and aggregation under flowing conditions of in vivo aspirin, heparin, and monoclonal antibody fragment against glycoprotein IIb-IIIa. *Circulation*. 1995;91(5):1354-62.
  45. Grabowski EF. Platelet aggregation in flowing blood at a site of injury to an endothelial cell monolayer: quantitation and real-time imaging with the TAB monoclonal antibody. *Blood*. 1990;75(2):390-8.